ERDC MSRC PET Preprint No. 01-31

A Comparison of Wave Hindcasts for a Gulf of Mexico Storm Using Quasi Time-Accurate and Time-Accurate Methods

by

Stephen F. Wornom
Richard Allard
Y. Larry Hsu

27 September 2001

Work funded by the Department of Defense
High Performance Computing Modernization Program
U.S. Army Engineer Research and Development Center
Major Shared Resource Center through

Programming Environment and Training

Supported by Contract Number: DAHC94-96-C0002
Computer Sciences Corporation

PET Preprint

A Comparison of Wave Hindcasts for a Gulf of Mexico Storm Using Quasi Time-Accurate and Time-Accurate Methods

Stephen F. Wornom
U.S. Army Engineer Research and Development Center
Major Shared Resource Center
Vicksburg, MS
and
Richard Allard and Y. Larry Hsu
Naval Research Laboratory
Coastal & Semi-Enclosed Seas Section
Stennis Space Center, MS

Abstract

SWAN (Simulating WAves Nearshore) is a third-generation wave model used to compute the spectra of random short-crested, wind-generated waves on Eulerian grids. SWAN has options to solve a stationary wave transport equation but most often is used to solve the nonstationary wave transport equation. Recently the term quasi time-accurate has been used to describe SWAN when the stationary transport equation is used for a nonstationary computation rather than the nonstationary transport equation. The quasi time-accurate version applies Message Passing Interface (MPI) techniques to solve in parallel the stationary wave transport equation for each data set of the time series. This study compares the quasi time-accurate results with the time-accurate results for a Gulf of Mexico storm that occurred in September 2000. The quasi time-accurate results in this study were obtained in 25 minutes on an Origin 3000 compared to 53 hours needed for the time-accurate results. Examination of root mean square norms, BIAS computations, and correlation plots at three National Data Buoy Center buoys shows that both methods give equivalent accuracy for this test case. Thus the MPI quasi time-accurate approach may play an important interim role for some cases until an efficient time-accurate version of SWAN becomes available.

Introduction

One of the major challenges in ocean modeling is the accurate prediction of nearshore wave conditions required for environmental impact studies of erosion and sediment transport and also equally important in naval operations. The SWAN (Simulating WAves Nearshore) code has been developed specifically for nearshore zones where finite-depth effects become important.

A major obstacle to routine use of the time-accurate version of SWAN is the large computational resources required. At present there is no parallel version of SWAN for high-performance computing platforms. Work on a parallel version is in its early stages, and encouraging progress has been recently reported by Campbell (2001) using OpenMP. Presently, the time-accurate version of SWAN is run on a single processor that can result

in very long execution times for some simulations. A case in point is the test case examined here, which required more than 50 hours of computing time on an Origin 3000 (O3K).

In order to arrive at a parallel version of the SWAN code, Wornom (2001) adopted a quasi time-accurate approach. In this approach, the time dependency enters the computation through time-varying boundary spectra, wind fields, and current fields; the wave action transport equation is solved as a stationary problem at each time interval rather than as a nonstationary problem. This approach has the advantage that the solution procedure changes from a sequential one to a single program with multiple data, where coarse-grain parallelism can be exploited using the message-passing interface (MPI) system.

The quasi time-accurate approach is one of the key features of the steady-state wave model (STWAVE), which solves a steady-state spectral wave equation. McKee-Smith et al. (2001) state that solving a steady-state equation "is appropriate for wave conditions that vary more slowly than the time it takes for waves to transit the computational grid. For wave generation, the steady-state assumption means that the winds have remained sufficiently long for the waves to attain fetch-limited or fully developed conditions." In general, STWAVE is applied on small areas with meshes extending not more than 5 kilometers (km) offshore (the direction from which the waves are arriving) and usually 10 km along shore. STWAVE propagates waves in one direction (toward the shore) and as the grids are small, the wind is uniform over the mesh as well as the boundary spectra imposed along the offshore boundary.

The purpose of this study is to compare the quasi time-accurate and the time-accurate version of SWAN for wave hindcasts of a Gulf of Mexico storm that occurred in September 2000 to assess the validity of the quasi time-accurate method. Therefore the general criteria set forth by McKee-Smith et al. (2001) as to when a stationary wave transport equation can be used may be not satisfied. The use of SWAN in the quasi time-accurate mode is also appealing, as wind fields can vary over the mesh, the boundary spectra need not be uniform, and waves can propagate in all directions. How the quasi time-accurate approach performs when applied to large domains and under extreme storm conditions is of great interest to the wave modeling community.

Test Case

The test case used in this study was a Gulf of Mexico storm that occurred in September 2000. Hsu et al. (2001) had previously studied this case using the time-accurate version of SWAN. As such, the bathymetry file and the boundary spectra files, as well as wind fields to drive the computations, were available along with computational results and wave data measurements at the test sites. When the MPI quasi time-accurate version became available, this seemed an ideal test case to compare the results for the two approaches. In the study of Hsu et al. (2001), a 219x159 grid with a 1 km mesh size was used employing 36 directional angles over a circle and 30 frequencies. Directional wave spectra were provided from a Mississippi Bight 1/12° regional WAM wave model run operationally by the Naval Oceanographic Office (NAVO). Figure 1 shows the detailed

bathymetry for the region studied and the locations of the WAM spectra applied to the SWAN outer boundaries. Time-varying winds were provided by the U.S. Navy's Coupled Ocean Atmosphere Mesoscale Prediction System (COAMPS) Central America grid. The COAMPS 10-meter winds were available on a 0.20° resolution grid with a temporal resolution of 6 hours. SWAN output was requested every 3 hours for the period 4-17 September 2001. A time-step of 12 minutes was used.

Computational Resources

The quasi time-accurate results were computed on the O3K at the U.S. Army Engineer Research and Development Center Major Shared Resource Center (ERDC MSRC) in Vicksburg, MS. A partial time-accurate calculation was made on the O3K to estimate that the total time-accurate computation would require approximately 53.8 hours.

The MPI quasi time-accurate implementation creates input files, named INPUT, and output files, named PRINT, on each process. A copy of the bathymetry field and wind fields are sent to each process. The availability of processes determines the throughput time. The ERDC MSRC O3K with 512 processors is well suited for the present MPI program.

Table 1 shows the wall clock times for using different numbers of MPI processes.

Table 1: Wall clock times

# Processes	Scheme	Wall clock time
1	time-accurate	53.8 hrs
2	quasi time-accurate	16.8 hrs
4	quasi time-accurate	8.8 hrs
29	quasi time-accurate	1.6 hrs
58	quasi time-accurate	42.6 min
116	quasi time-accurate	25.7 min

The speedups for the quasi time-accurate version and wall times using different numbers of processes on the O3K are shown in Figures 2a-b.

Evaluation Methods

The quasi time-accurate and the time-accurate methods were examined using root mean square norms (RMS) of the significant wave heights, mean wave directions, and the average wave periods at three test sites. Correlation plots were also examined. Table 2 gives the water depths at the test sites.

Table 2: Water depths at test sites

Test site	Water depth (m)
NDBC 44007	13.0
NDBC 42040	237.7
NDBC 42042	33.0

The RMS norms were computed using the following formula:

$$\mathrm{RMS}(\mathrm{H}) = \sqrt{\frac{1}{\mathrm{N}}\sum_{1}^{\mathrm{N}}(\mathrm{H}_c - \mathrm{H}_d)(\mathrm{H}_c - \mathrm{H}_d)} \Big/ \frac{1}{\mathrm{N}}\sum_{1}^{\mathrm{N}}\mathrm{H}_d \qquad (0.1)$$

H represents the significant wave height, the mean wave direction, or the average wave period. The subscript "c" is for computation and "d" for the data (measurements). N is the number of points. For the computation of the RMS and BIAS, only the points that were in the range 4 September 2000 0-UTC to 17 September 2000 0-UTC were used. The BIAS in the solutions was computed using the expression

$$\mathrm{BIAS}(\mathrm{H}) = \frac{1}{\mathrm{N}}\sum_{1}^{\mathrm{N}}\mathrm{H}_c - \mathrm{H}_d \qquad (0.2)$$

The plotted mean wave directions were scaled to the range 0 to 360 degrees using the following expressions:

$$if\ \ \theta_i \geq 360;\ \theta_i = \theta_i - 360 \qquad (0.3)$$

$$if\ \theta_i \leq 0;\ \theta_i = \theta_i + 360 \qquad (0.4)$$

For the computation of the RMS for the mean wave directions, the following expressions were used:

$$\begin{aligned} &\Delta\theta = \theta_c - \theta_d \\ &\text{if } \Delta\theta \geq 180; \Delta\theta = 360 - \Delta\theta \\ &\text{if } \Delta\theta \leq -180; \Delta\theta = -(360 + \Delta\theta) \end{aligned} \qquad (0.5)$$

Results

Significant wave heights

The RMS norms for the significant wave heights at the four test sites and the BIAS in the solutions are shown in Tables 3-4. Table 3 gives the RMS norms for the significant wave heights for both the time-accurate (ta) and the quasi time-accurate results. The norms are approximately the same with the time-accurate being slightly smaller than the quasi time-accurate norms. Table 4 shows the BIAS to be smaller for the quasi time-accurate results in general. The correlation coefficients for the significant wave heights are shown in Table 5. The correlation coefficient is defined as

$$\sigma(\mathrm{H}) = 1 - \mathrm{RMS}(\mathrm{H})$$

Columns 2-3 show the correlation between the computations and the data (measurements). The correlations between the two computations are given in column 4. The correlations with the data are approximately the same. The correlations between the two computations are much higher than each computation with the data.

Table 3: RMS values for the significant wave heights

Test site	Time-accurate	Quasi time-accurate
NDBC 44007	0.424	0.432
NDBC 42042	0.384	0.410
NDBC 42040	0.341	0.345

.

Table 4: BIAS in the significant wave heights

Test site	Time-accurate	Quasi time-accurate
NDBC 44007	-0.154	-0.151
NDBC 42042	0.011	0.009
NDBC 42040	0.000	0.015

Table 5: Correlation coefficients for the significant wave heights

Test site	Time-accurate/data	Quasi ta/data	Time-accurate/quasi ta
NDBC 42007	0.5758	0.5679	0.7609
NDBC 42042	0.6163	0.5904	0.7954
NDBC 42040	0.6591	0.6548	0.8222

NDBC 42007 - Figures 3a-d show comparisons of the computed results with the data at the National Data Buoy Center (NDBC) 42007 buoy. The time-accurate and the quasi time-accurate results for the significant wave heights (Hmo) agree well with each other; there are no major differences between the two solutions. Correlation plots obtained when computations are plotted vs. the measurements and against each other are shown in Figures 4a-b. Good correlation is measured by how close the data fall on the line indicated as “zero bias.” Also shown on these plots are linear fits to the data. Figure 4b shows that the Hmo results for the computations correlate very well with one another. Neither of the computations correlates well with the measurements (Figure 4a). The linear data fits are negligibly different.

NDBC 42040 - Comparisons between the computed significant wave heights and the measurements at the NDBC 42040 buoy are shown in Figures 5a-d. In general, the computations agree reasonably well with the measurements. The differences between the computations are very small. The agreement between the computed results and the data and the computed results themselves are shown in Figures 6a-b.

NDBC 42042 - Comparisons between the significant wave heights and the measurements at the NDBC 42042 are shown in Figures 7a-d. The agreement between the computations is extremely good. The agreement between the computations and the data is reasonably

good, but peaks in the wave heights are underpredicted. Correlation plots are shown in Figures 8a-b.

Mean wave directions

The RMS norms for the mean wave directions at the three test sites and the BIAS in the solutions are shown in Tables 6-7. Table 6 gives the RMS norms for the mean wave directions for both the time-accurate and the quasi time-accurate results. The norms are approximately the same with the time-accurate being slightly smaller than the quasi time-accurate norms. Table 7 shows the BIAS to be smaller for the quasi time-accurate results at two of the three test sites. The correlations between the two computations given in Table 8 show similar trends as the significant wave heights.

Table 6: RMS values for the mean wave directions

Test site	Time-accurate	Quasi time-accurate
NDBC 44007	36.173	39.702
NDBC 42040	63.031	63.879
NDBC 42042	62.098	61.296

Table 7: BIAS in the mean wave directions

Test site	Time-accurate	Quasi time-accurate
NDBC 44007	-11.883	-8.973
NDBC 42040	-30.801	-30.049
NDBC 42042	-35.048	-35.022

Table 8: Correlation coefficients for the mean wave directions

Test site	Time-accurate/data	Quasi ta/data	Time-accurate/quasi ta
NDBC 42007	0.5758	0.5679	0.7609
NDBC 42042	0.6163	0.5904	0.7954
NDBC 42040	0.6591	0.6548	0.8222

NDBC 42007 - Figures 9a-d show comparisons of the computed mean wave directions with the data at the NDBC 42007 buoy. The time-accurate and the quasi time-accurate results for the mean wave directions are approximately the same; there is no noticeable difference between the two solutions. The correlation between the two computations is shown in Figure 10.

NDBC 42040 - Comparisons between the computed mean wave directions and the measurements at the NDBC 42040 buoy are shown in Figures 11a-d. In general, the computations agree reasonably well with the measurements. The differences between the computations are very small. Figure 12 shows good correlation between the computations.

NDBC 42042 - Comparisons between the mean wave directions and the measurements at the NDBC 42042 are shown in Figures 13a-d. The agreement between the computations

is good as can be observed in Figure 14. The agreement between the computations and the data is reasonable, but the peaks in the mean wave directions are underpredicted.

Average wave period

The RMS norms for the average wave period at the four test sites and the BIAS in the solutions are shown in Tables 9-10. Table 11 gives the RMS norms for the average wave period for both the time-accurate and the quasi time-accurate results. The norms are approximately the same with the time-accurate being slightly smaller than the quasi time-accurate norms. Table 10 shows the BIAS to be approximately the same with both methods, with each underpredicting the average wave period. The correlations between the two computations given in Table 11 show similar correlation trends as the significant wave heights.

Table 9: RMS values for the average wave period

Test site	Time-accurate	Quasi time-accurate
NDBC 44007	0.259	0.281
NDBC 42042	0.213	0.227
NDBC 42040	0.170	0.171

.

Table 10: BIAS in the average wave period

Test site	Time-accurate	Quasi time-accurate
NDBC 44007	-0.816	-0.942
NDBC 42042	-0.246	-0.348
NDBC 42040	-0.463	-0.395

Table 11: Correlation coefficients for the average wave period

Test site	Time-accurate/data	Quasi ta/data	Time-accurate/quasi ta
NDBC 42007	0.7410	0.7185	0.8072
NDBC 42042	0.7865	0.7726	0.8536
NDBC 42040	0.8305	0.8286	0.8770

NDBC 42007 - Figures 15a-d show comparisons of the computed results with the data at the NDBC 42007 buoy. The time-accurate and the quasi time-accurate results for the average wave period are approximately the same with both underpredicting the average wave period. The quasi time-accurate results do exhibit noticeable spikes in the computed wave period. The correlation between the computations is shown in Figure 16. Good correlation is noted between the two methods.

NDBC 42040 - Comparisons between the computed average wave period and the measurements at the NDBC 42040 buoy are shown in Figures 17a-d. In general, the computations agree reasonably well with the measurements. The differences between the

computations are very small. The correlation between the computations is seen to be reasonably good in Figure 18.

NDBC 42042 - Comparisons between the average wave period and the measurements at the NDBC 42042 are shown in Figures 19a-d. The agreement between the computations is reasonably good. Figure 20 shows the correlation between the computations to be good.

Conclusions

This study compared the wave hindcasts using the quasi time-accurate and the time-accurate version of the SWAN code for a Gulf of Mexico storm that occurred in September 2000. This test case was previously studied using the time-accurate version of the SWAN code as the nearshore wave model. The directional wave spectra used at the SWAN seaward boundaries were provided by NAVO from a Mississippi Bight 1/12° regional WAM wave model run. Time-varying winds used to drive the WAM and SWAN wave models were provided by COAMPS Central America grid. The COAMPS 10-meter winds were available on a 0.20° resolution grid with a temporal resolution of 6 hours. The purpose of this study was to compare the quasi time-accurate version of SWAN with the time-accurate version to determine its accuracy on large domains and under extreme storm conditions. Examination of RMS norms, BIAS in the solutions, and correlation plots for the significant wave heights, mean wave directions, and average wave periods at three test sites shows the following:

1. The differences in the computed wave heights, mean wave directions, and average wave periods at the three NDBC buoys were very small.
2. The advantage of the MPI quasi time-accurate version lies in its efficiency. The quasi time-accurate results were obtained in 25 minutes compared with 53.8 hours for the time-accurate version on the O3K at the ERDC MSRC.
3. The MPI quasi time-accurate approach can be extended to the time-accurate version using data partitioning where MPI is applied over the partitions at each time-step rather than over the data. Thus the OpenMP time-accurate version being developed by Campbell can be used inside each partition. This would result in an efficient dual-level parallelism implementation.
4. In the final analysis, the SWAN user must decide whether the time-accurate results requiring more than 50 hours of computation are more valuable than the quasi time-accurate results obtained in 25 minutes. Both methods will find their proper place in the wave modeler’s toolbox.

Acknowledgments

This work was supported in part by a grant of computer time from the Department of Defense High Performance Computing Modernization Program at the ERDC MSRC in Vicksburg, MS. The first author would like to thank Dr. Robert Jensen of the Coastal and Hydraulics Laboratory at ERDC for suggesting and supporting the various SWAN Programming Environment and Training (PET) studies as a part of the PET technology transfer effort. The first author would also like to acknowledge many fruitful discussions with Erick Rogers of the Naval Research Laboratory (NRL) at the Stennis Space Center concerning the SWAN code and for his suggesting the quasi time-accurate approach.

References

Campbell, Timothy (2001), NAVO PET Principal Investigator and developer of an OpenMP parallel version of the time-accurate SWAN code, personal communication.

Hsu, Y. Larry, Allard, Richard A., and Mettlach, Theodore R.,
"Wave Model Validation for the Northern Gulf of Mexico Littoral Initiative,"
submitted as a NRL Report, September 2001.

Wornom, Stephen F., Welsh, David J.S., and Bedford, Keith W.,
"On Coupling the SWAN and WAM Wave Models for Accurate Nearshore Wave Predictions," *Coastal Engineering Journal,* Vol. 43 No. 3, September 2001.

McKee-Smith, Jane, Sherlock, Ann R., and Resio, Don,
"STWAVE: Steady-State Spectral Wave Model Users' Manual for STWAVE Version 3.0," U.S. Army Engineer Research and Development Center
Coastal and Hydraulics Laboratory Report ERDC/CHL SR-01-1.

Wornom, Stephen F., "An MPI Quasi Time-Accurate Approach for Nearshore Wave Prediction Using the SWAN Code," ERDC MSRC Preprint 01-29.

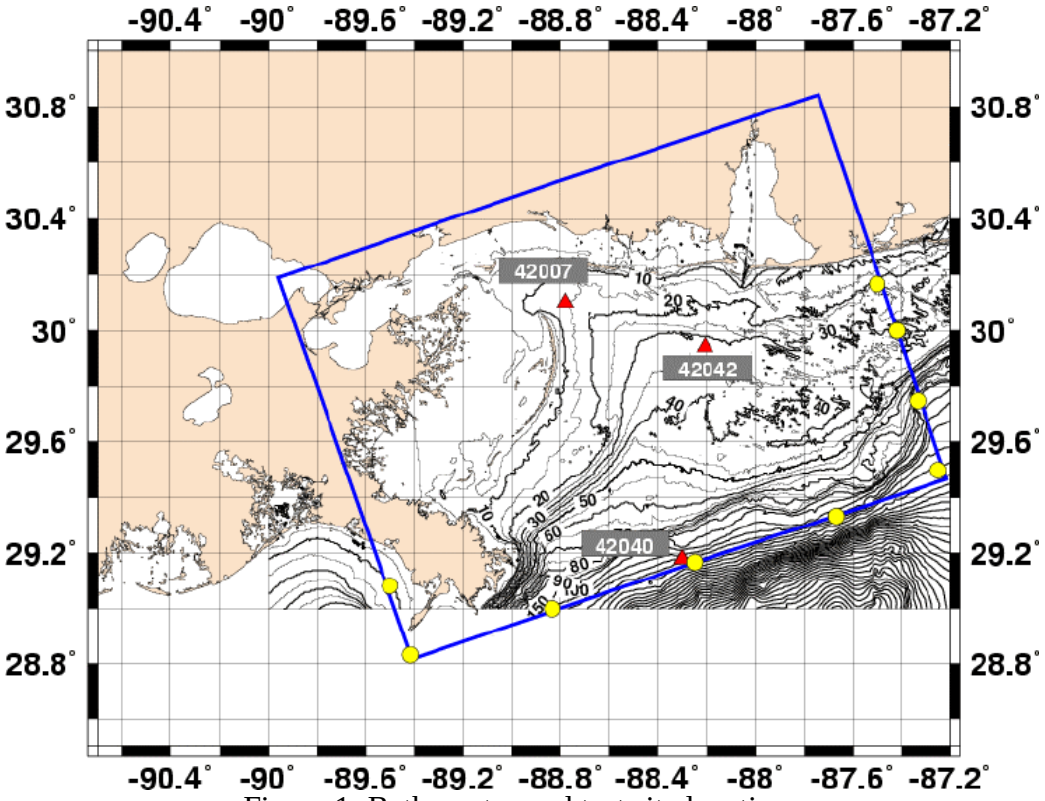

Figure 1: Bathymetry and test site locations

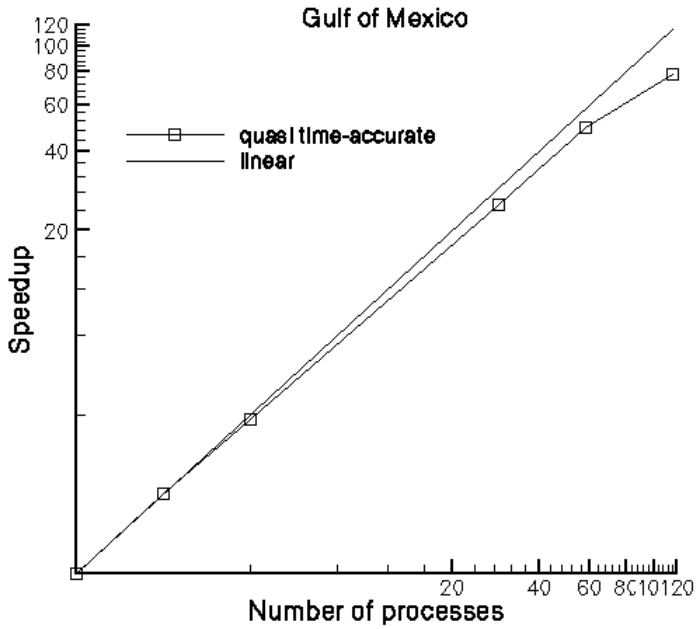

Figure 2a: Speedups vs. number of processes

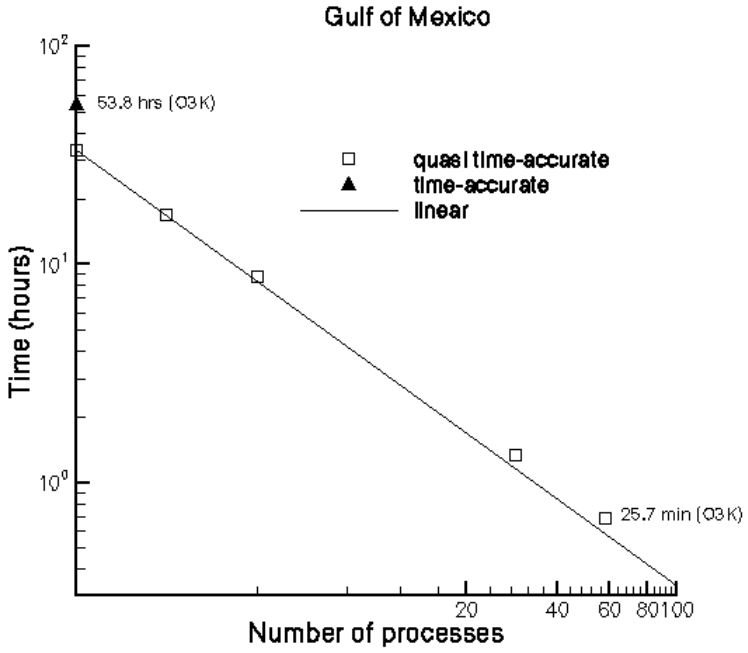

Figure 2b: Wall clock times vs. number of processes

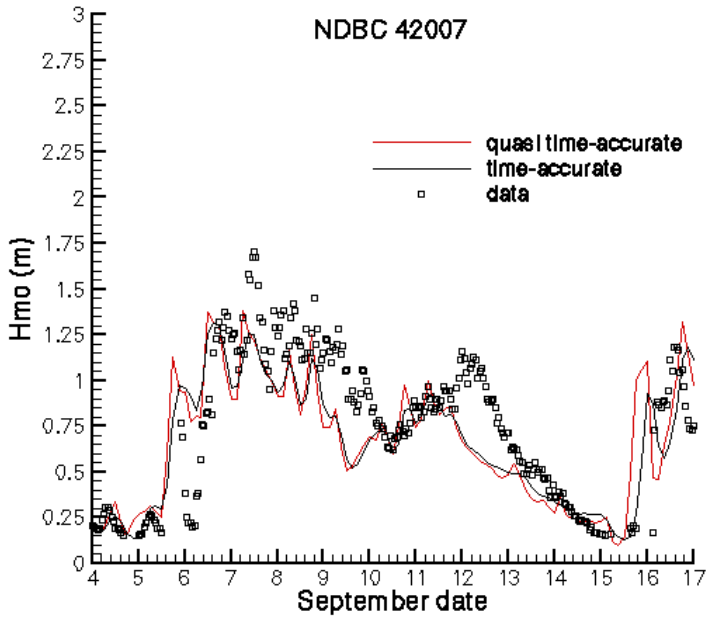

Figure 3: Time-series for the Hmo at NDBC 42007
a) Computations and data

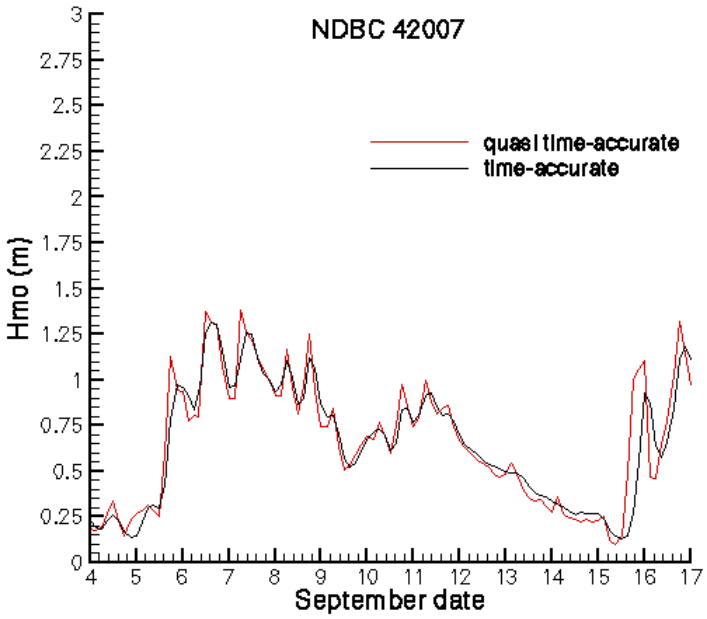

Figure 3b: Computations only

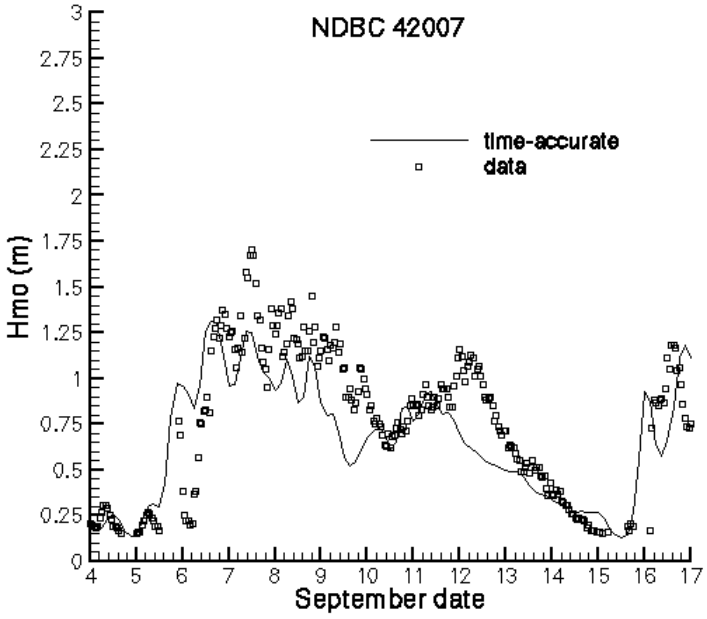

Figure 3c: Time-accurate results with data

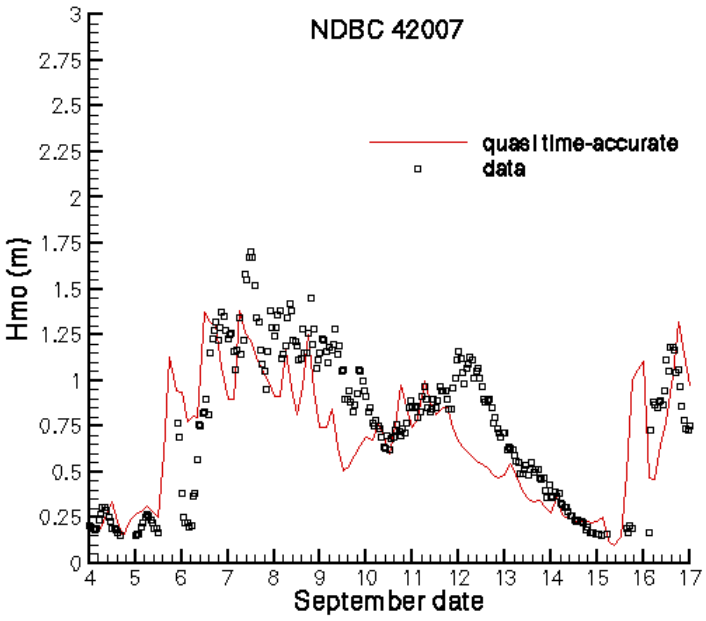

Figure 3d: Quasi time-accurate results with data

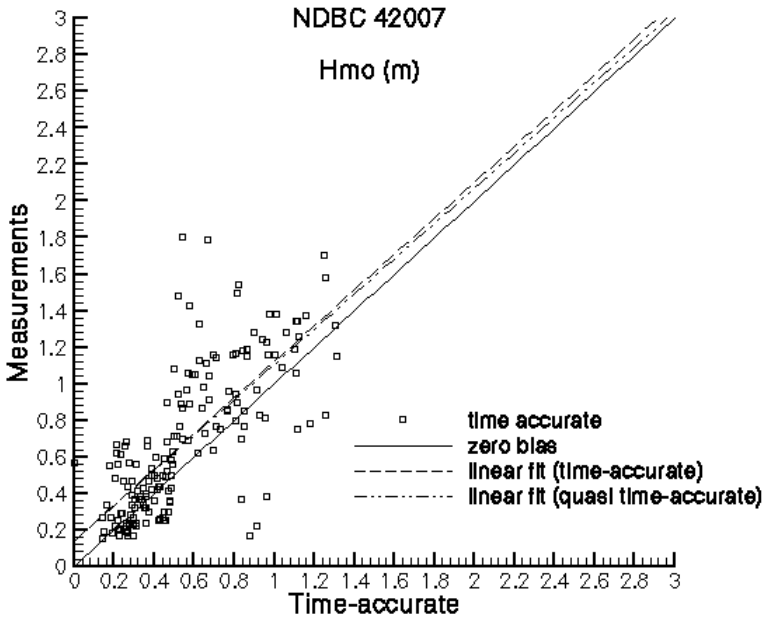

Figure 4a: Correlation with Hmo data at NDBC 42007

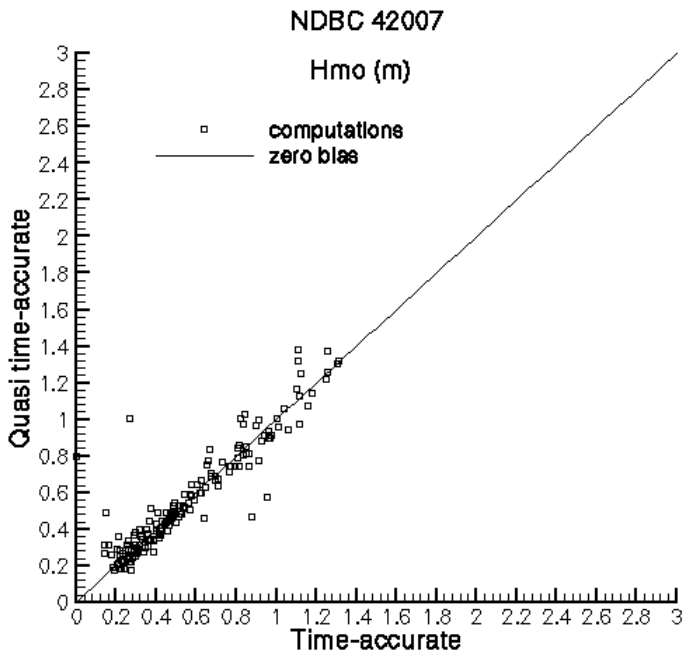

Figure 4b: Correlation with computation Hmo values at NDBC 42007

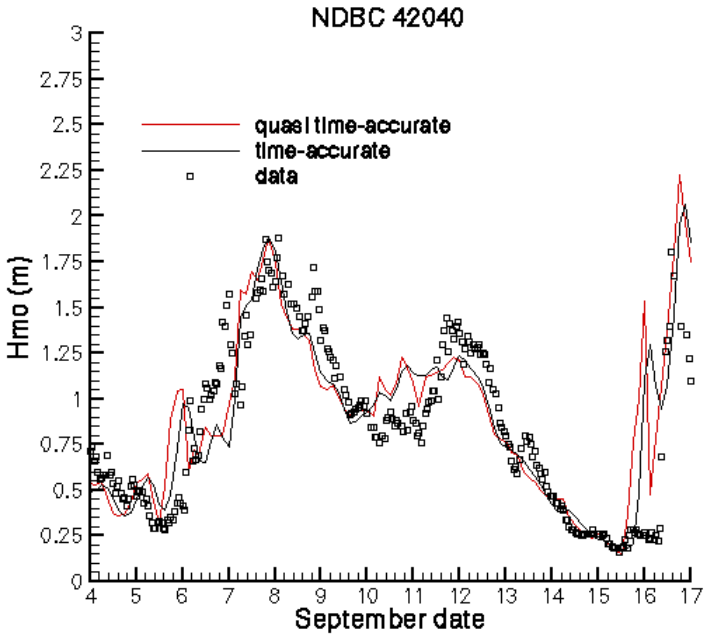

Figure 5: Time-series for the Hmo at NDBC 42040
a) Computations and data

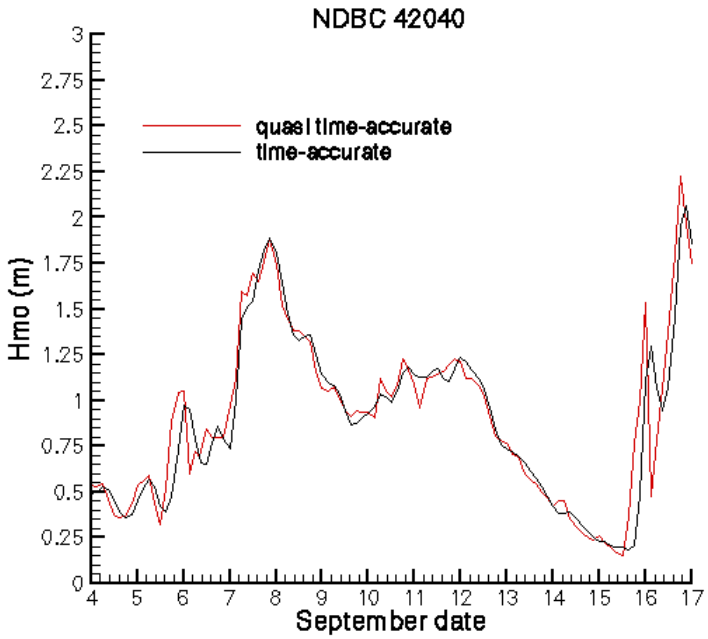

Figure 5b: Computations only

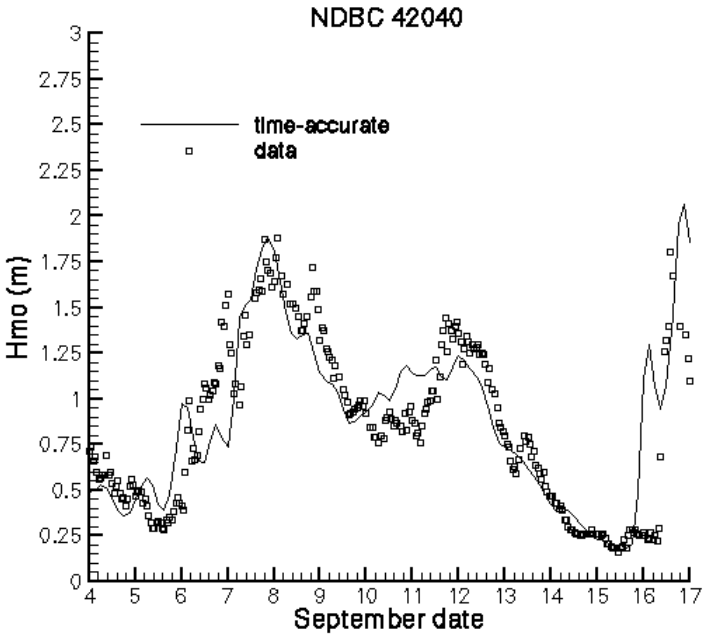

Figure 5c: Time-accurate results with data

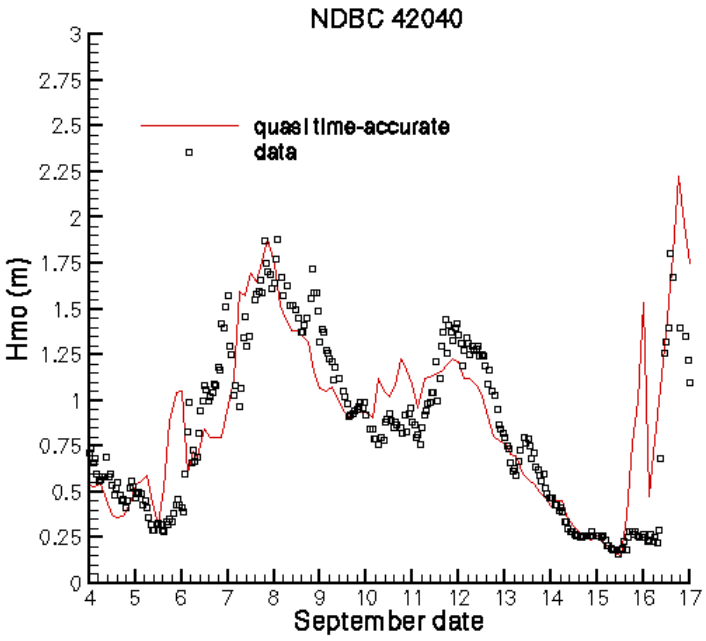

Figure 5d: Quasi time-accurate results with data

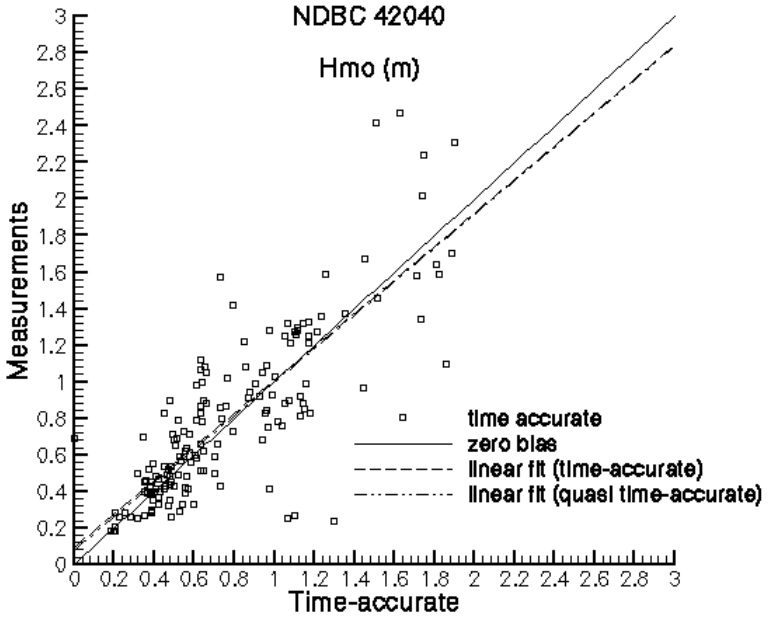

Figure 6a: Correlation with Hmo data at NDBC 42040

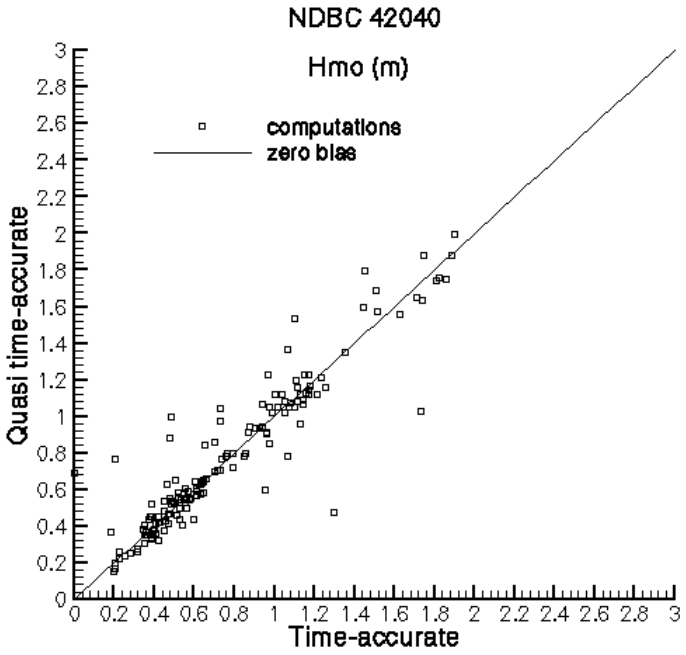

Figure 6b: Correlation with computation Hmo values at NDBC 42040

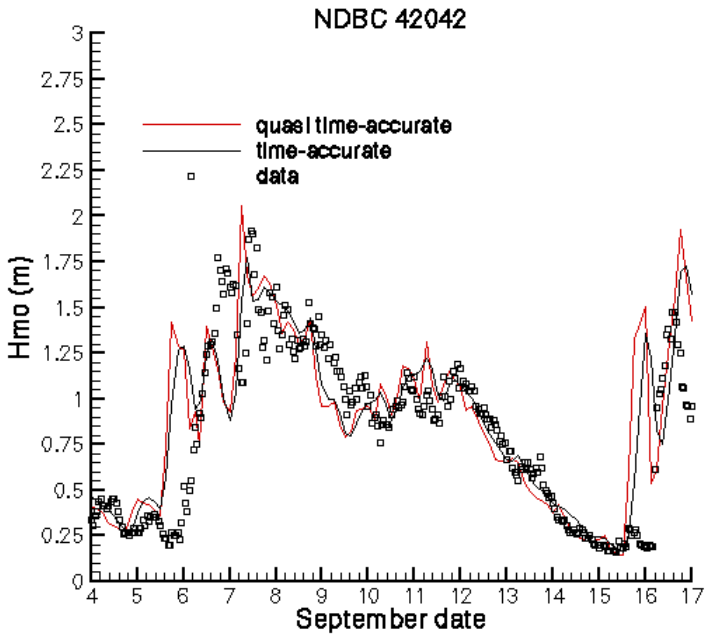

Figure 7: Time-series for the Hmo at NDBC 42042
a) Computations and data

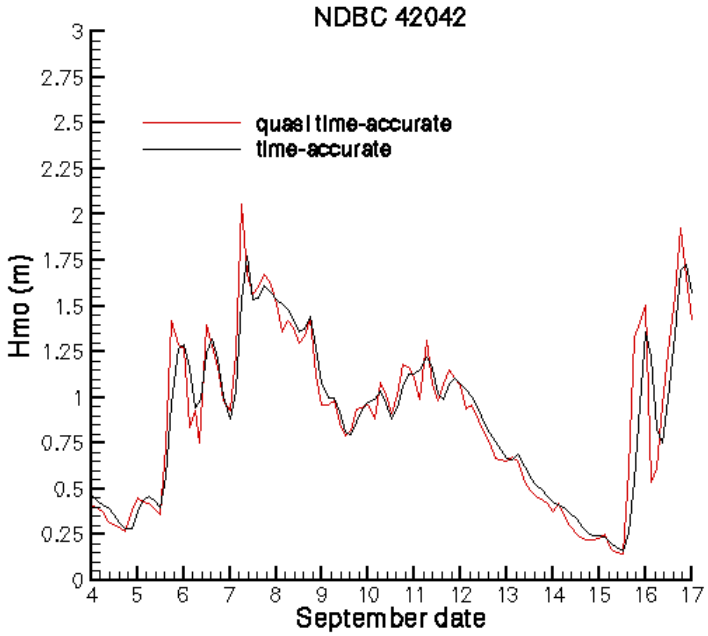

Figure 7b: Computations only

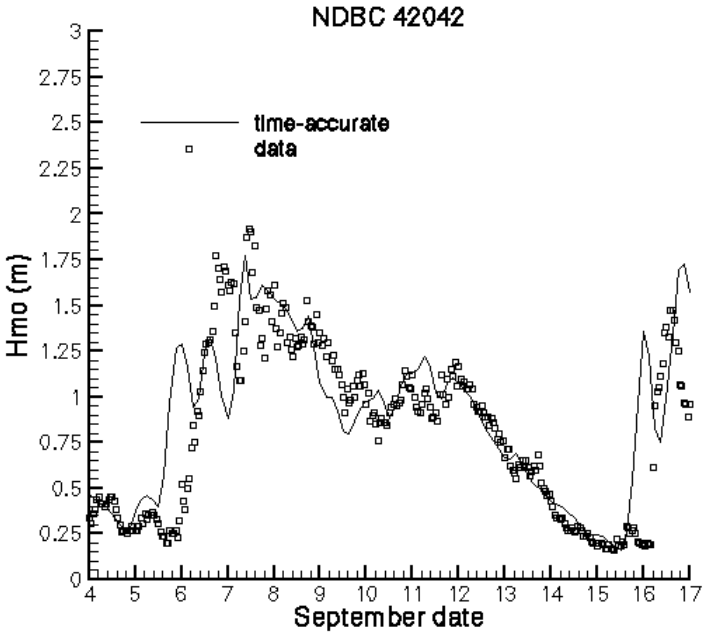

Figure 7c: Time-accurate results with data

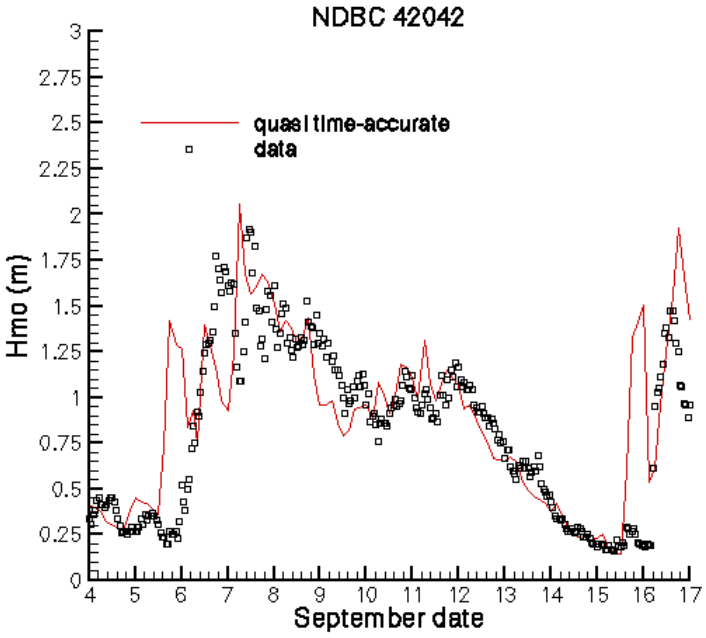

Figure 7d: Quasi time-accurate results with data

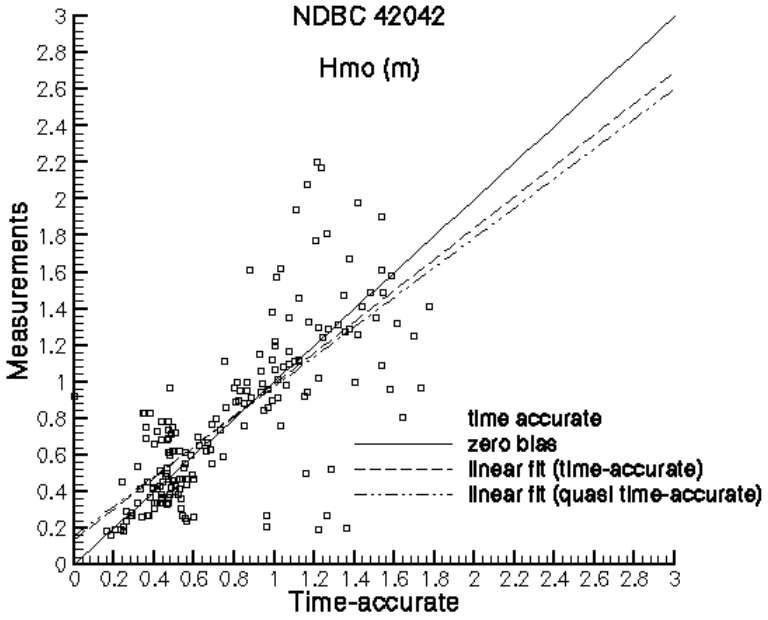

Figure 8a: Correlation with Hmo data at NDBC 42042

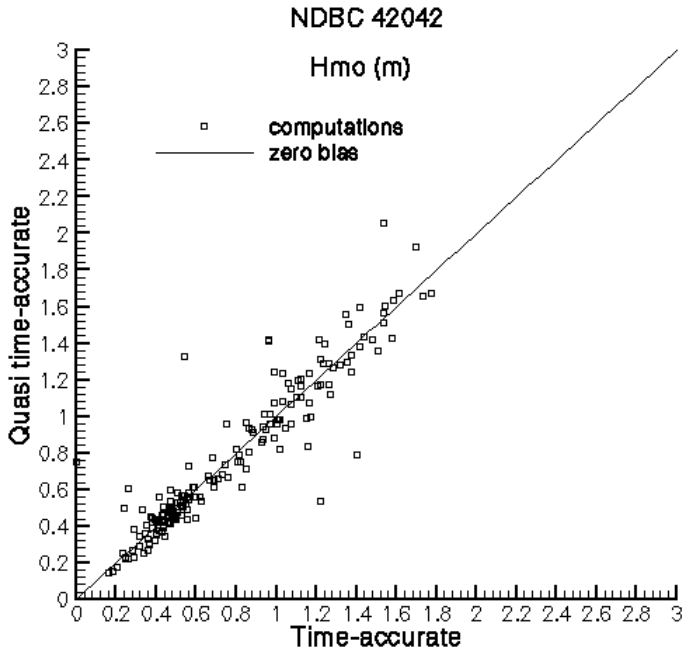

Figure 8b: Correlation with computed Hmo values at NDBC 42042

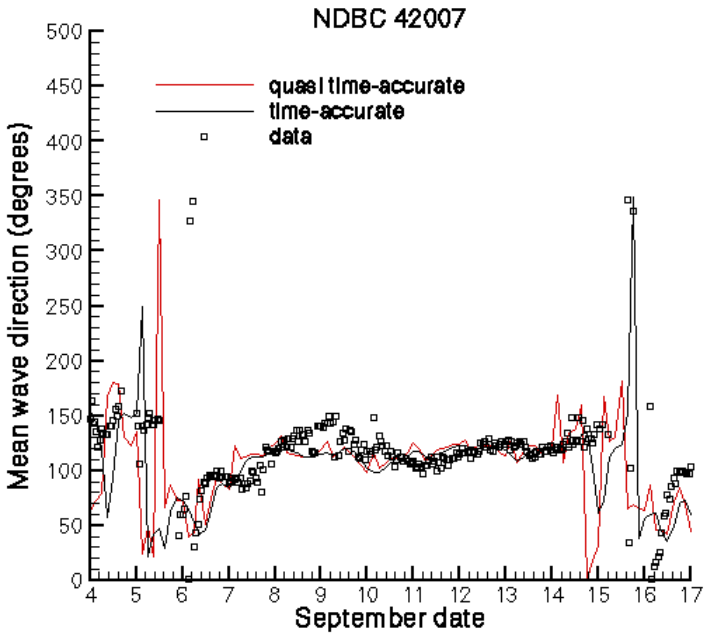

Figure 9: Time-series for the mean wave direction at NDBC 42007
a) Computations and data

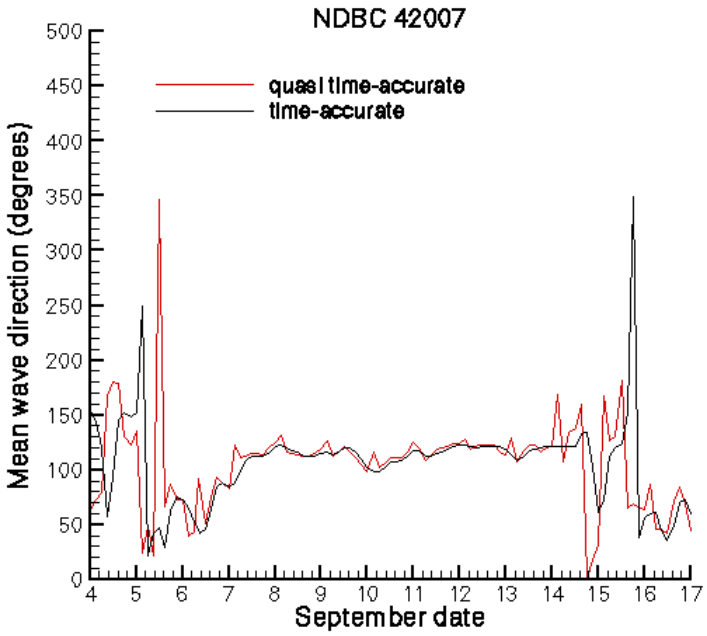

Figure 9b: Computations only

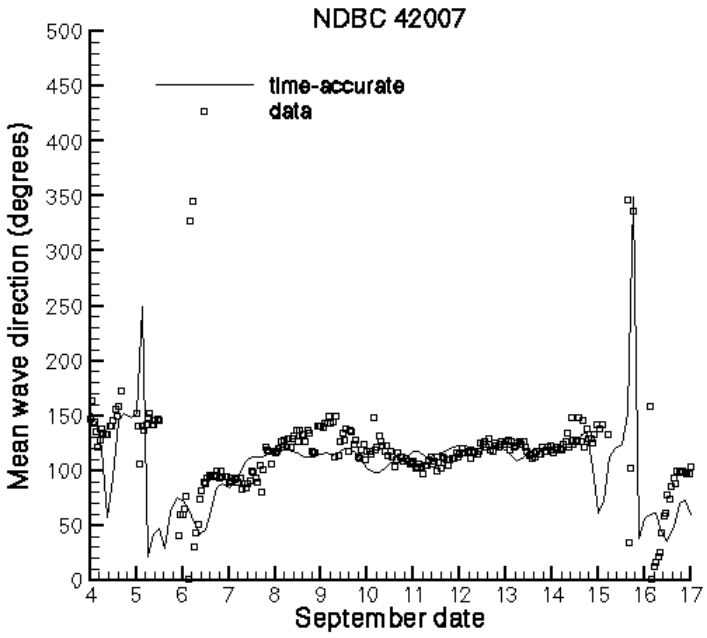

Figure 9c: Time-accurate results with data

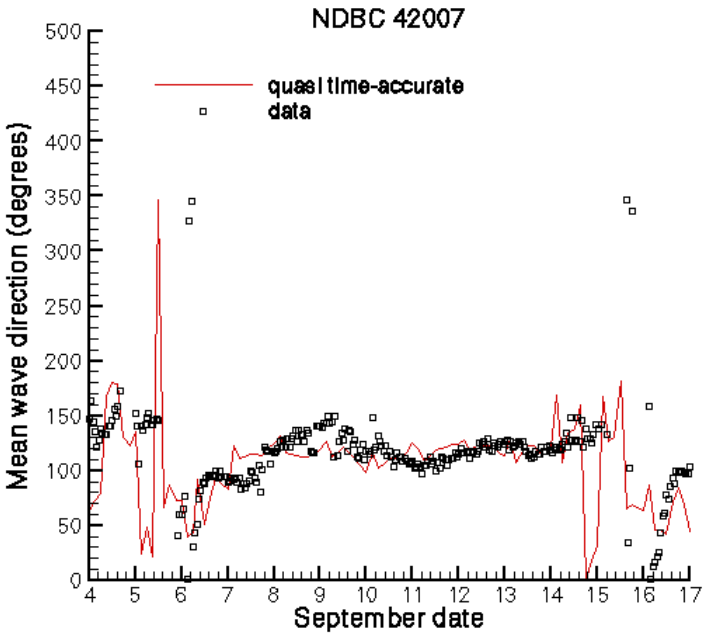

Figure 9d: Quasi time-accurate results with data

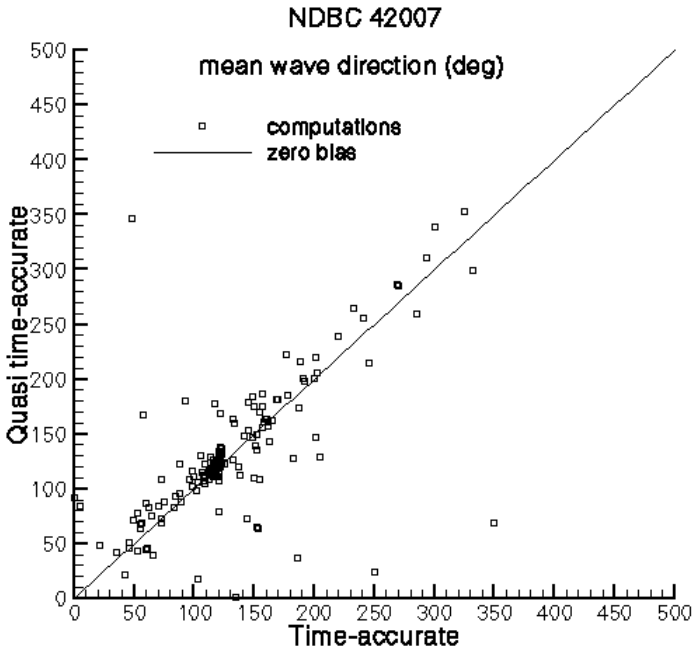

Figure 10: Computation correlation for mean wave direction data at NDBC 42007

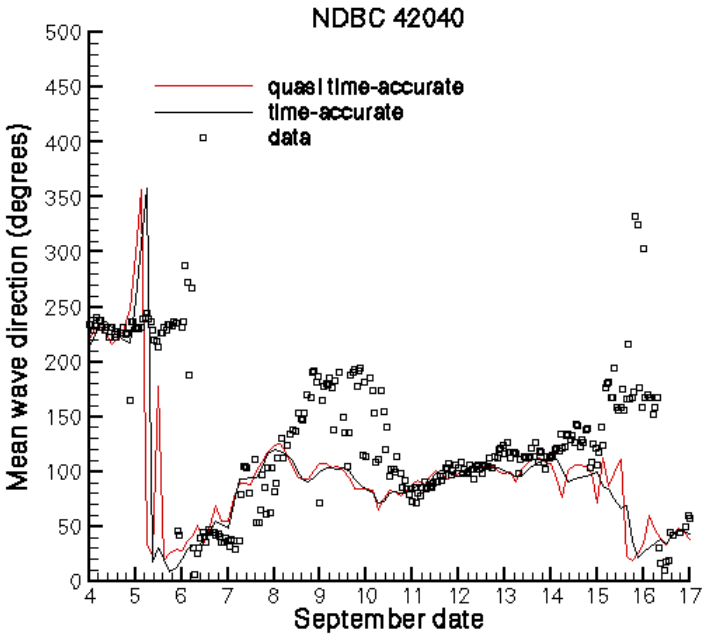

Figure 11: Time-series for the mean wave direction at NDBC 42040
a) Computations and data

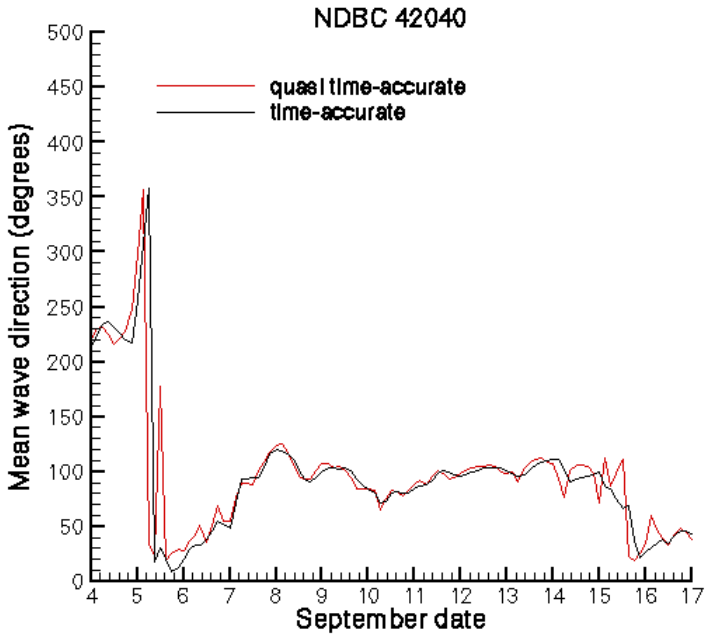

Figure 11b: Computations only

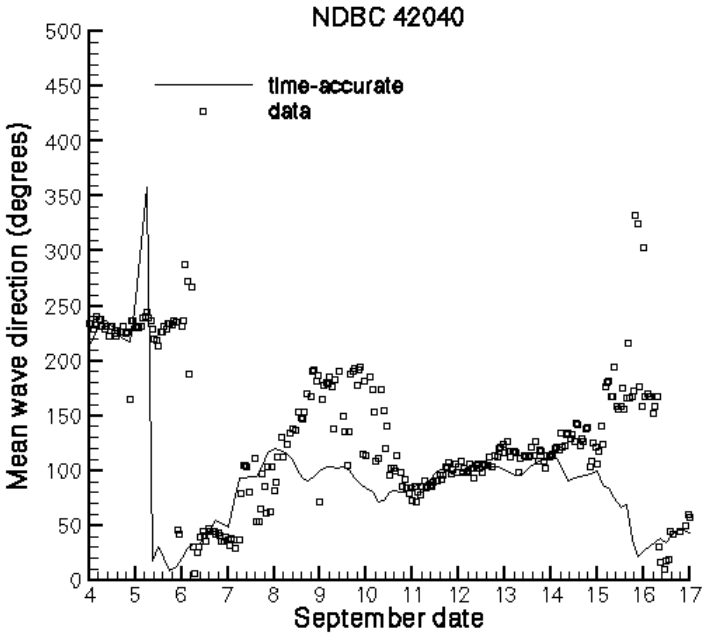

Figure 11c: Time-accurate results with data

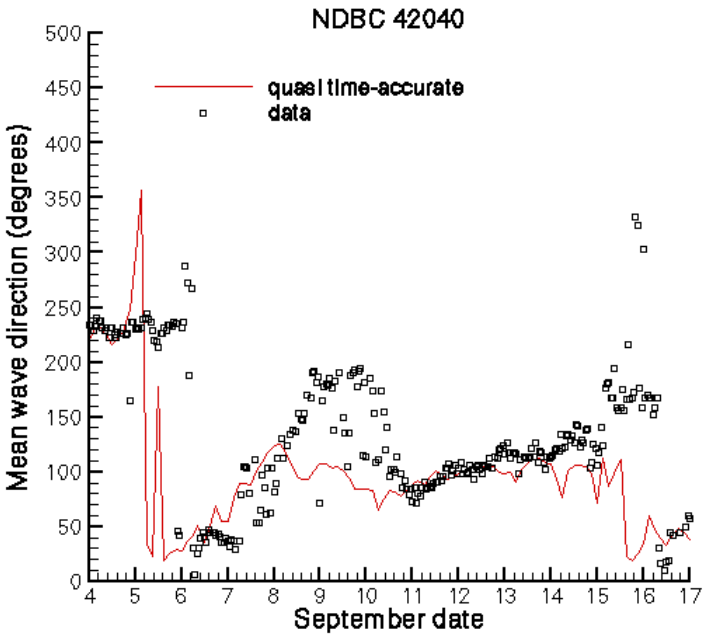

Figure 11d: Quasi time-accurate results with data

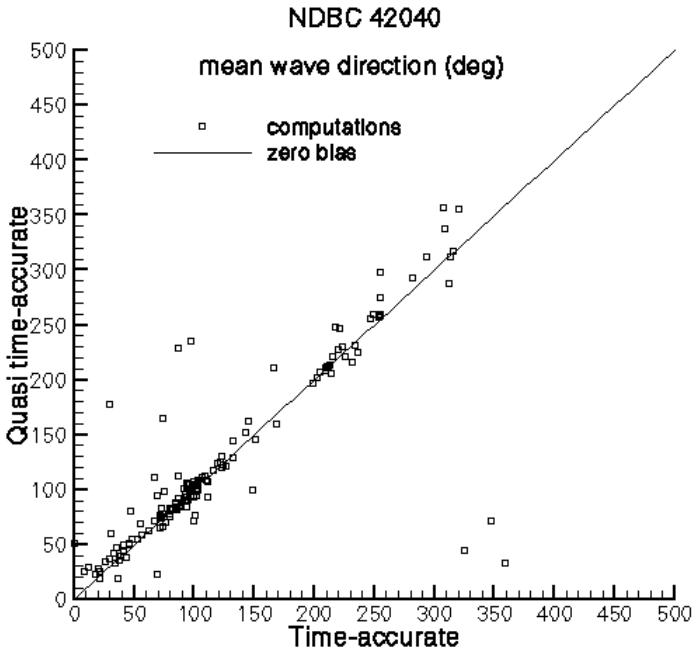

Figure 12: Computation correlation for mean wave direction data at NDBC 42040

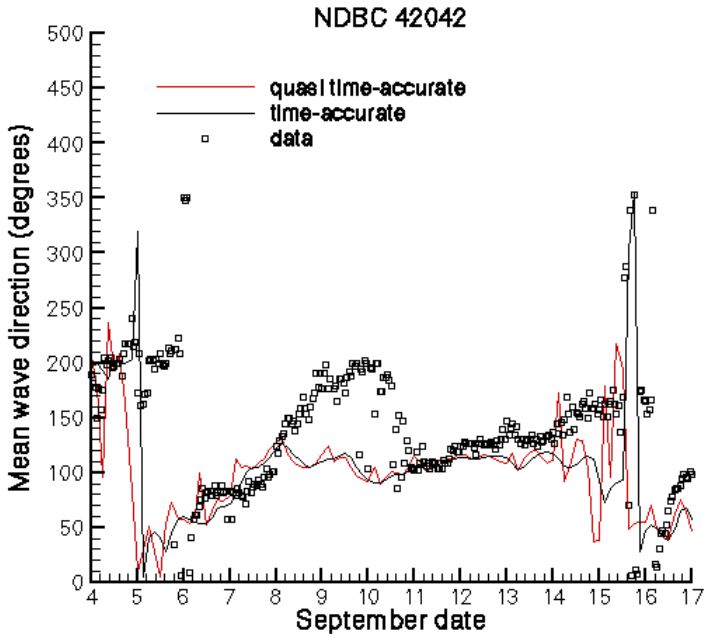

Figure 13: Time-series for the mean wave direction at NDBC 42042
a) Computations and data

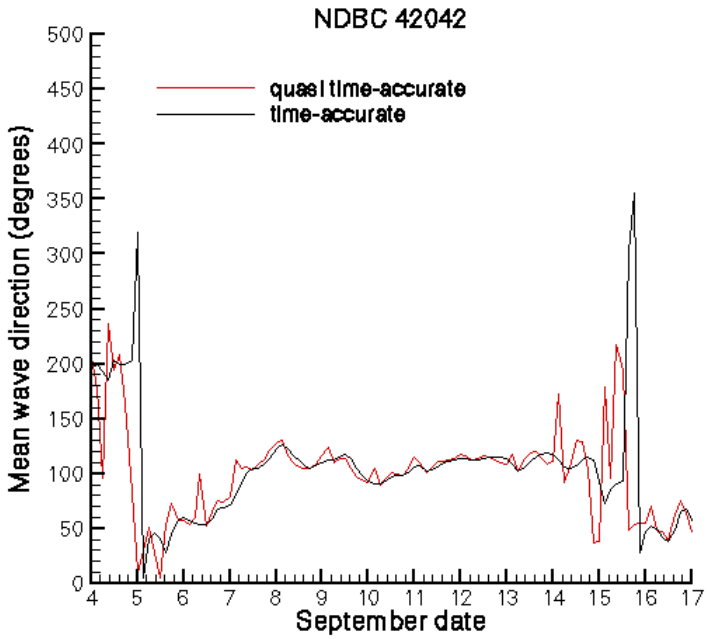

Figure 13b: Computations only

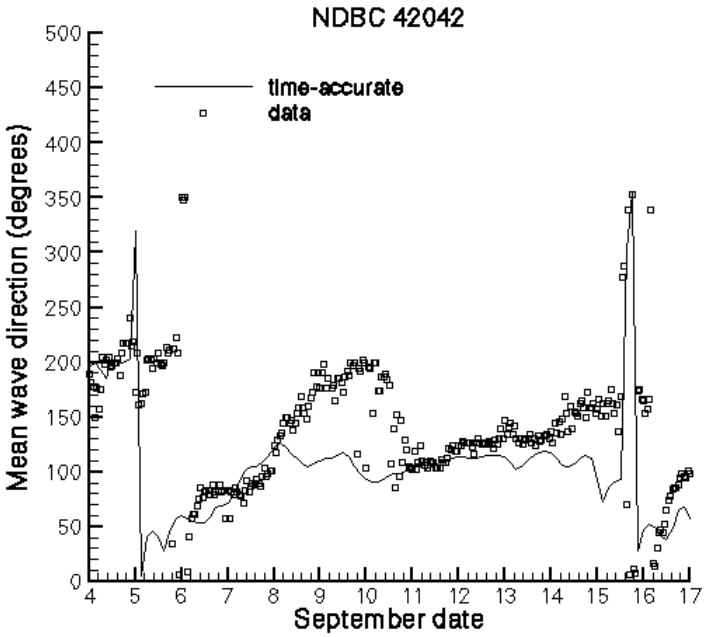

Figure 13c: Time-accurate results with data

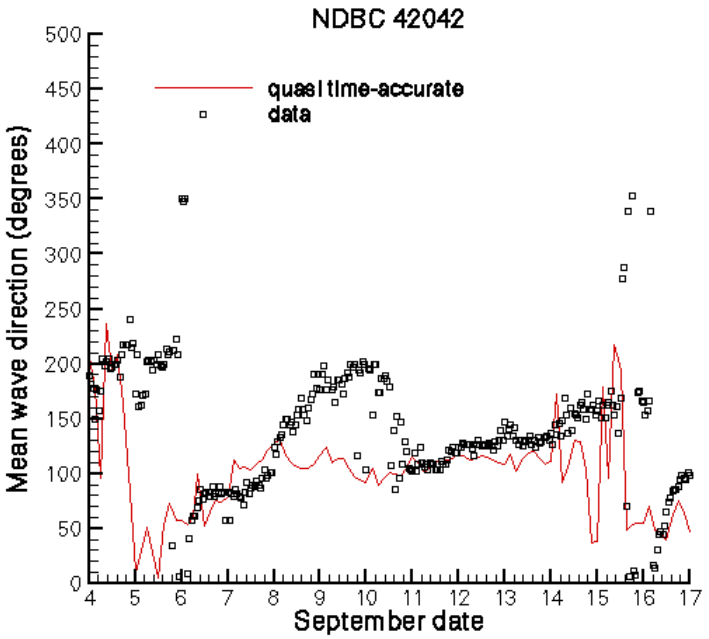

Figure 13d: Quasi time-accurate results with data

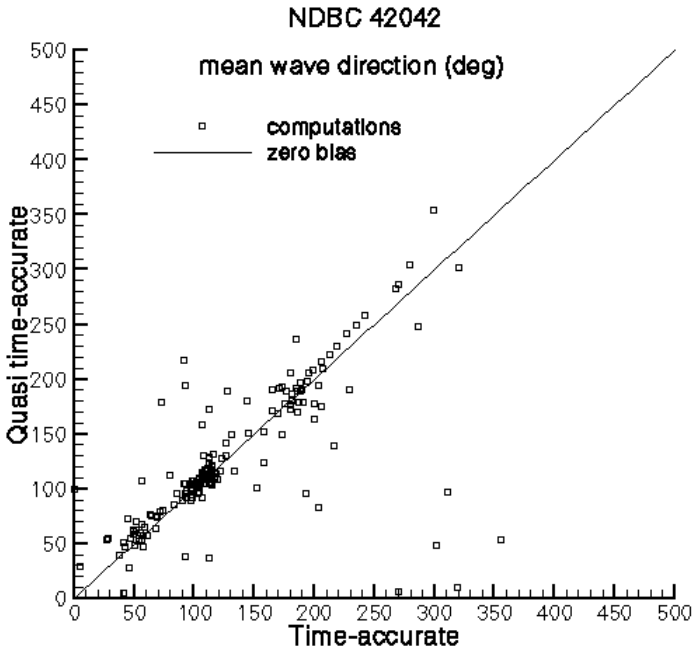

Figure 14: Computation correlation for mean wave direction data at NDBC 42042

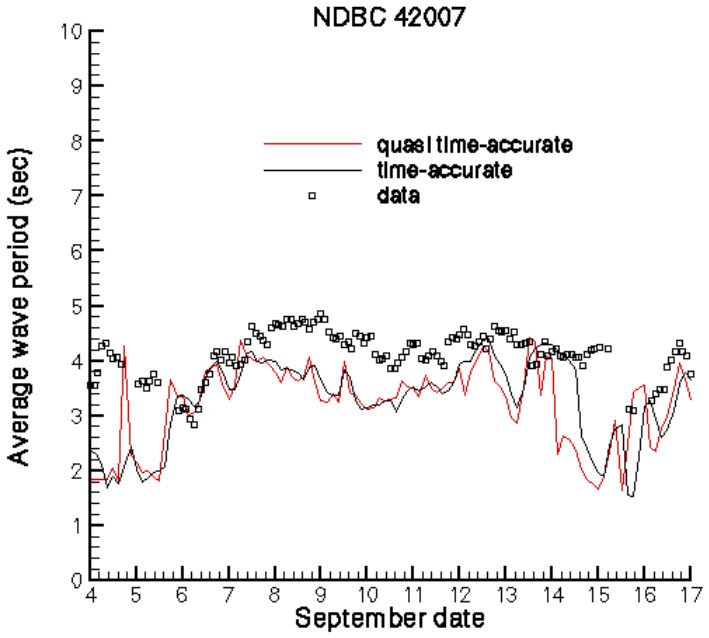

Figure 15: Time-series for the average wave period at NDBC 42007
a) Computations and data

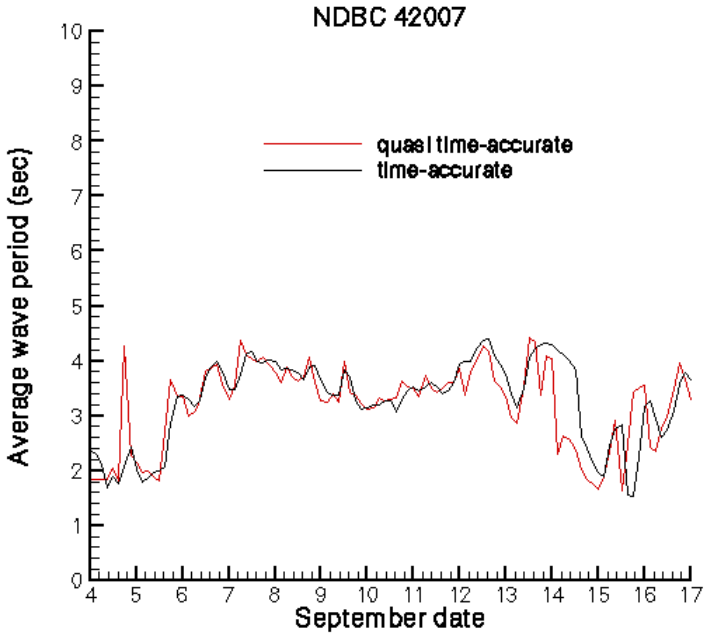

Figure 15b: Computations only

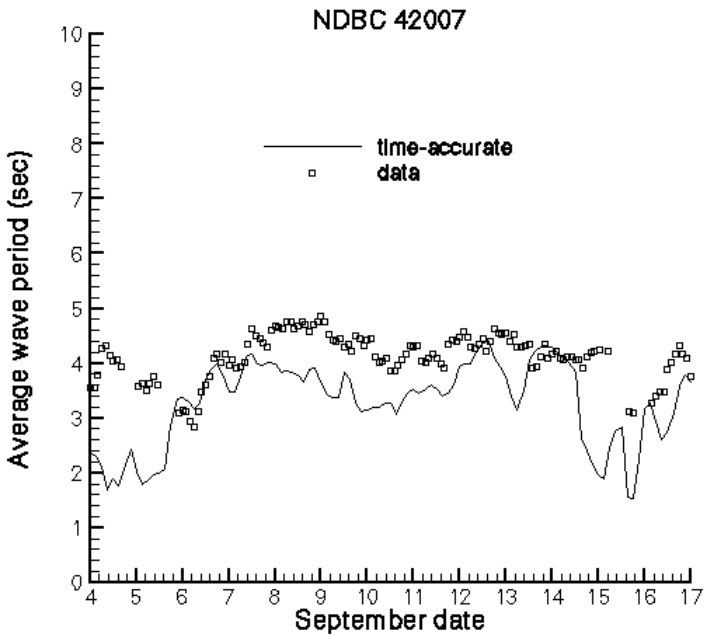

Figure 15c: Time-accurate results with data

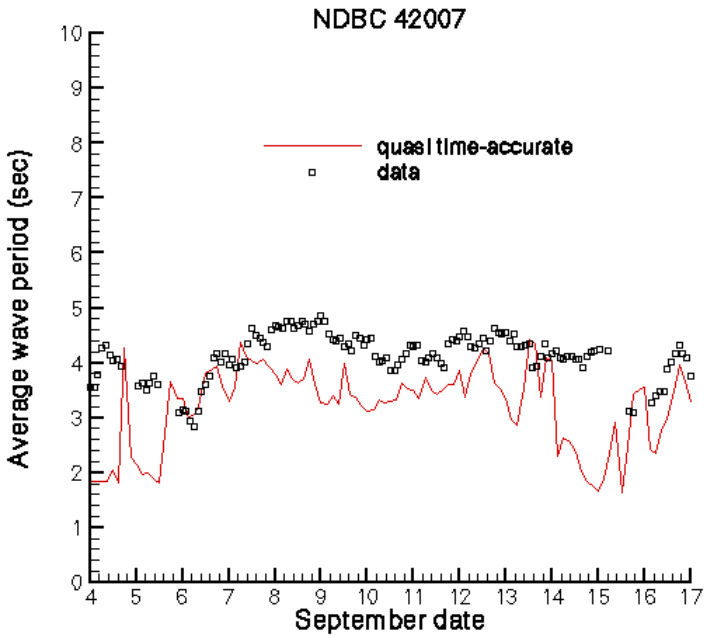

Figure 15d: Quasi time-accurate results with data

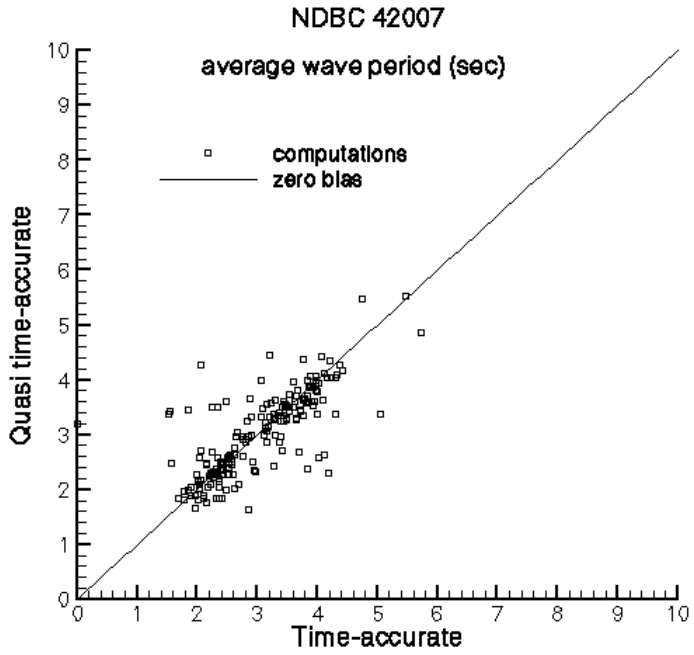

Figure 16: Computation correlation for average wave period data at NDBC 42007

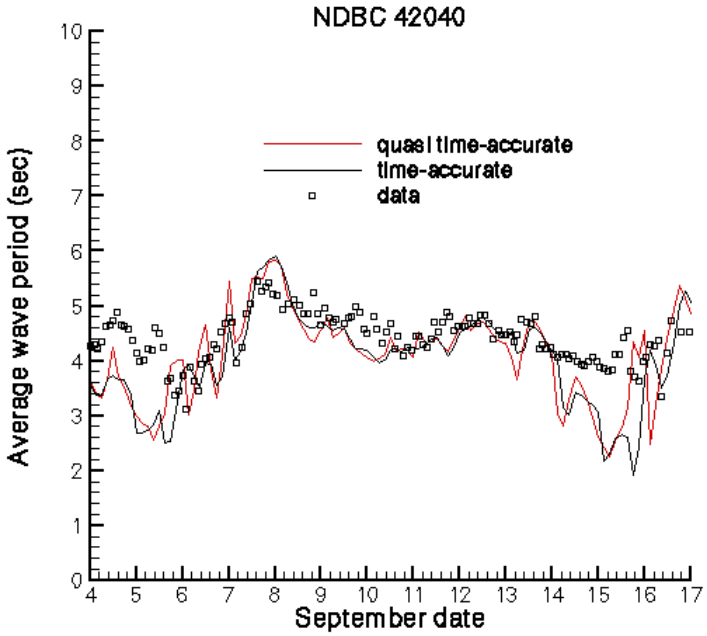

Figure 17: Time-series for the average wave period at NDBC 42040
a) Computations and data

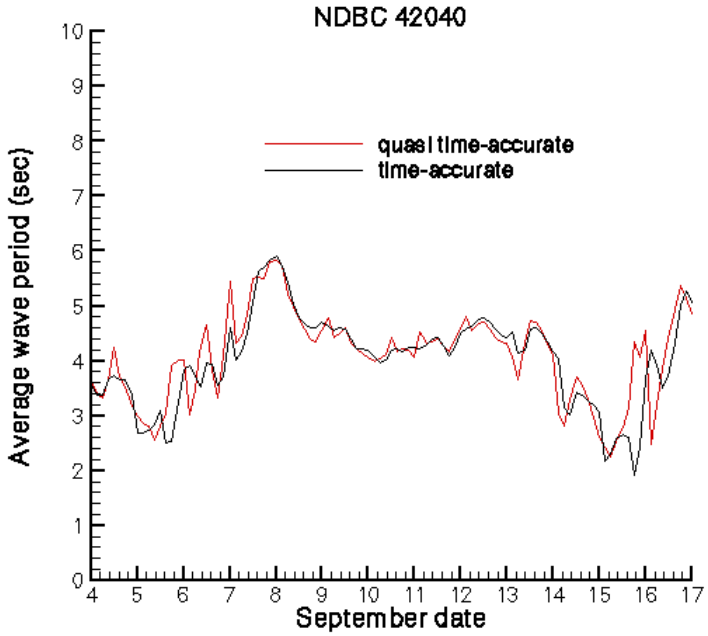

Figure 17b: Computations only

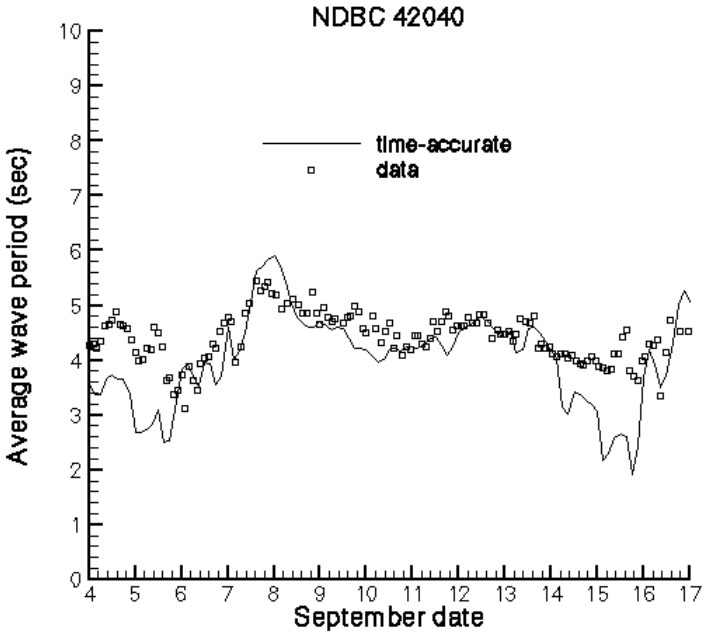

Figure 17c: Time-accurate results with data

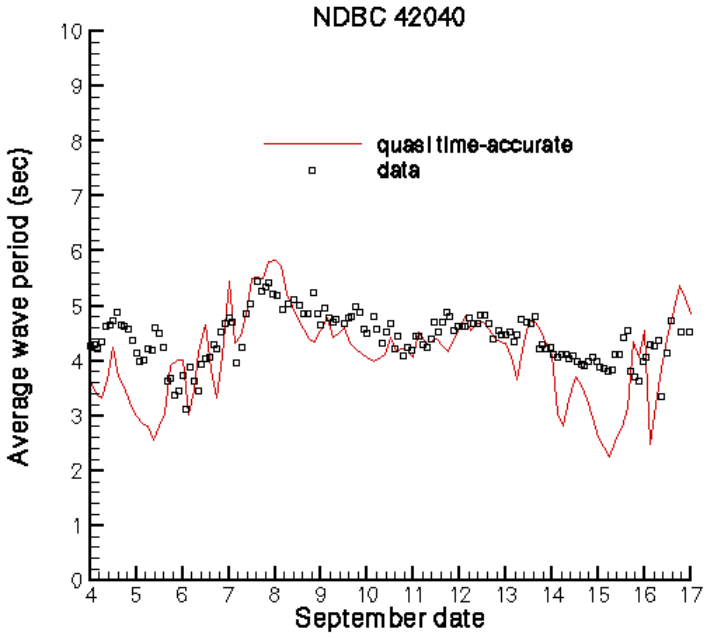

Figure 17d: Quasi time-accurate results with data

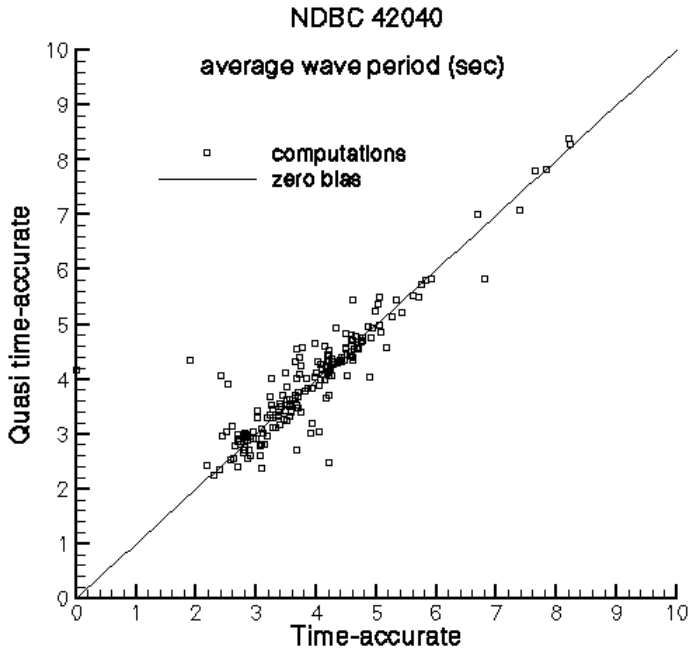

Figure 18: Computation correlation for average wave period data at NDBC 42040

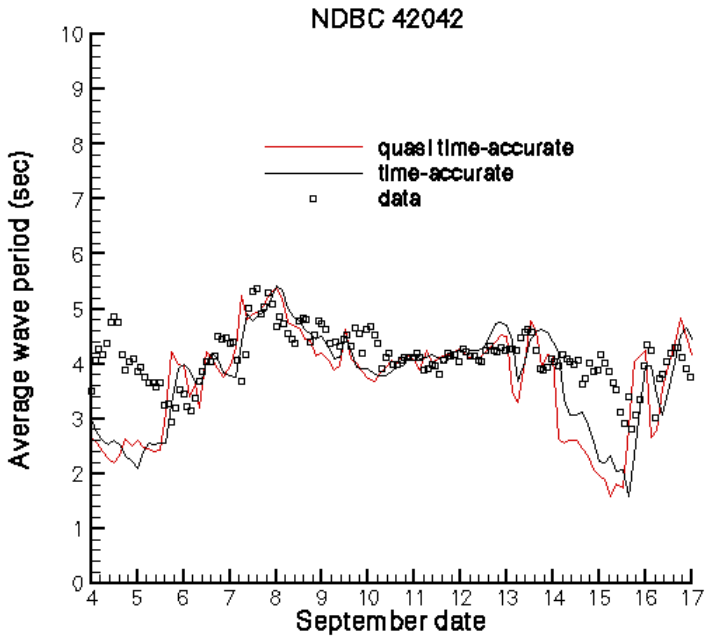

Figure 19: Time-series for the average wave period at NDBC 42042
a) Computations and data

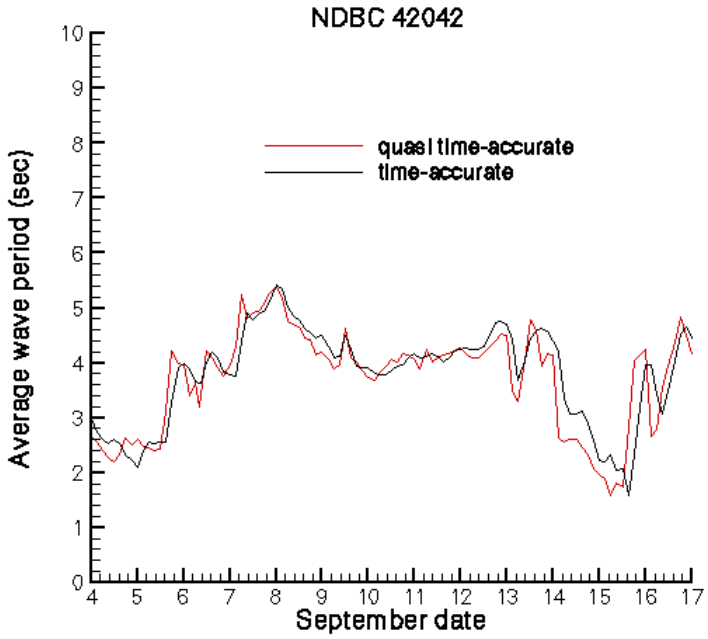

Figure 19b: Computations only

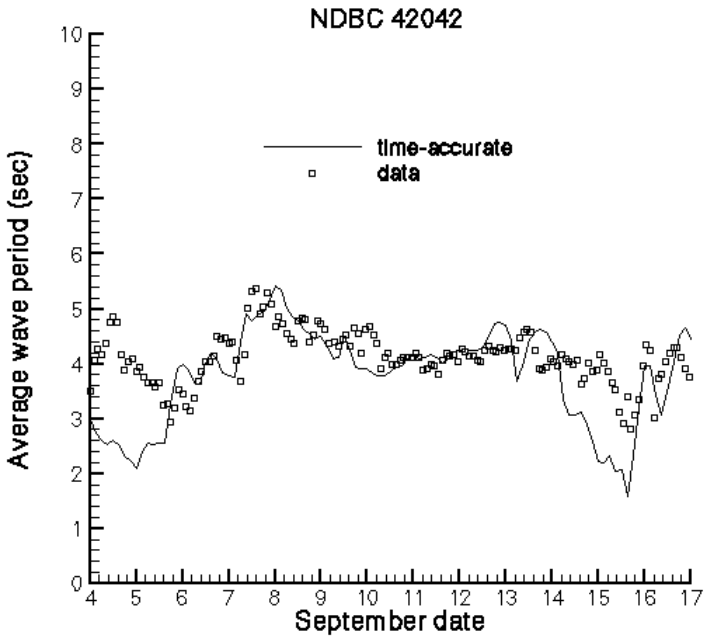

Figure 19c: Time-accurate results with data

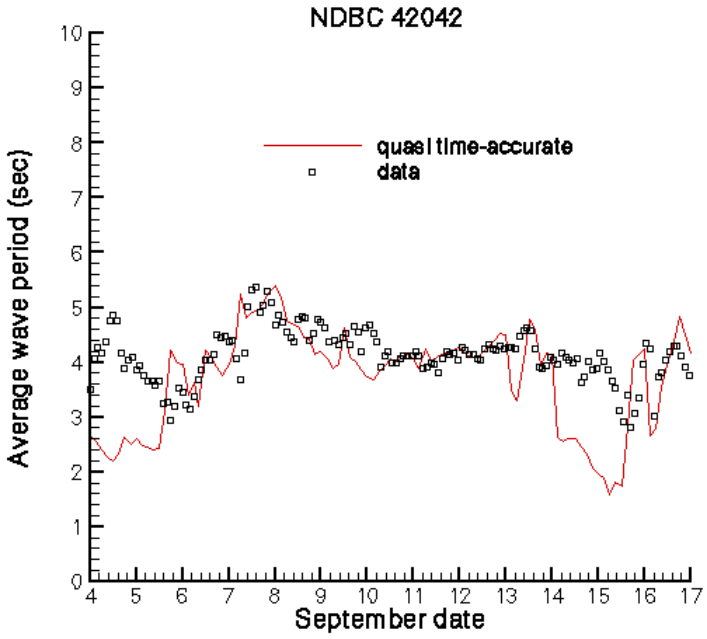

Figure 19d: Quasi time-accurate results with data

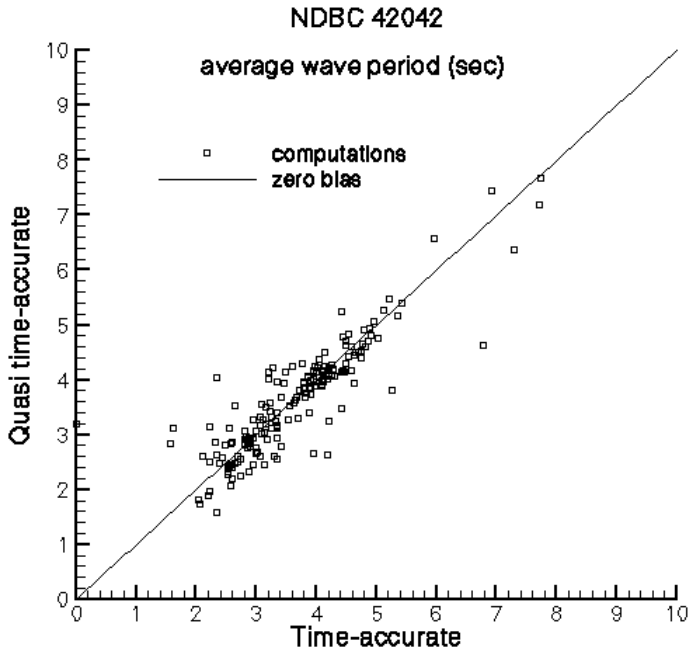

Figure 20: Computation correlation for average wave period data at NDBC 42042